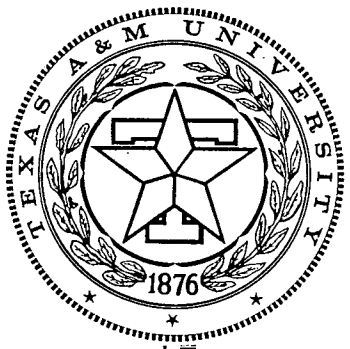

TEXAS
TRANSPORTATION
INSTITUTE

TEXAS
HIGHWAY
DEPARTMENT

COOPERATIVE
RESEARCH

THEORY, RESISTANCE OF A DRILLED SHAFT FOOTING TO OVERTURNING LOADS

in cooperation with the
Department of Transportation
Federal Highway Administration
Bureau of Public Roads

RESEARCH REPORT 105-1
STUDY 2-5-67-105
DESIGN OF FOOTINGS FOR MINOR SERVICE STRUCTURES

THEORY, RESISTANCE OF A DRILLED SHAFT FOOTING TO OVERTURNING LOADS

by

Don L. Ivey
Associate Research Engineer

Research Report Number 105-1

Design of Footings for Minor Service Structures

Research Study Number 2-5-67-105

Sponsored by
THE TEXAS HIGHWAY DEPARTMENT
in cooperation with
The U. S. Department of Transportation
Federal Highway Administration
Bureau of Public Roads

February, 1968

TEXAS TRANSPORTATION INSTITUTE
Texas A&M University
College Station, Texas

ACKNOWLEDGMENTS

The theory described by this paper was developed as the initial phase of a study sponsored jointly by the Texas Highway Department and the Bureau of Public Roads. Liason was maintained through Mr. D. L. Hawkins and Mr. H. D. Butler, contact representatives for the Texas Highway Department, and through Mr. Robert J. Prochaska of the Bureau of Public Roads.

The opinions, findings, and conclusions expressed in this publication are those of the author and not necessarily those of the Bureau of Public Roads.

INTRODUCTION

The wide use of drilled shaft footings to support service structures necessary for the functioning of a highway system has focused attention on the highly conservative design procedures presently in use. Thc foundations for structures such as signboards, strain poles, and lighting poles should be designed using factors of safety consistent with the relative importance of the particular structure. Present design methods do not allow this since the real factor of safety is not indicated by the ultra-conservative methods of analysis. The development of a reliable analysis technique will result in considerable economy through the use of reasonable factors of safety.

This is the first of a series of reports to be written concerned with the design of these footings. It shows in detail the theoretical development on which the subsequent reports will be based. The second report in this series will provide a comparison of the theory with model tests and the third report will present a "Tentative Design Procedure" for the practicing engineer charged with the design of signboard and pole structures.

THEORETICAL DEVELOPMENT

Statement of Problem

Consider the drilled shaft footing of a circular cross-section shown in Figure 1. The loads that are of interest are the horizontal loads and overturning moments at the top of the footing (at the surface of the ground). The vertical load on the footing is not large enough to make a vertical failure mode a possibility. Any combination of horizontal loads and overturning moments can be resolved into a single load acting some distance above the top of the footing. This treatment will be based on the resistance of these footings to a horizontal load (P) acting a distance (H) above the top of the footing.

As the load P is applied the footing begins to rotate about point O, developing soil stresses on the various contact surfaces until balancing resistances have developed that prevent further movement of the footing. Initially these stress developments are somewhat elastic in nature, by which we imply that the soil around the footing is in a state of elastic equilibrium, ". . . an indefinitely small increase of the stress difference produces no more than an infinitely small increase in the strain."[1] As the load P approaches the maximum load the footing can withstand, a soil condition is finally approached that can be described using the following definitions: "... an infinitely small increase of the stress differences produces a steady increase of the corresponding strain. This phenomenon constitutes plastic flow. The flow is preceded by a state of plastic equilibrium."[2]

The plastic equilibrium condition is reached on various points of the footing at different degrees of rotation. For example, the top of the footing would undergo the most lateral movement for a given rotation, thereby forcing the adjacent soil into the plastic flow condition first. This soil then yields as rotation continues with no further increase in stress. The soil at an increased depth, progressively closer to the point of rotation, goes through plastic equilibrium and into the plastic flow condition.[3] Finally, (at maximum load) most of the soil adjacent to the advancing boundaries of the footing is in a state of plastic flow.

The forces developed on the footing are shown in Figure 2. Most of the prior treatments of this problem have considered only the horizontal forces, F_{xa} and F_{xb}, which are the major forces resisting overturning. These treatments have in general fallen into two groups; either highly empirical (Seiler,[4] Patterson,[5] and Downs[6]) or those with highly conservative theoretical assumptions (Anderson,[7] Will,[8] Williams,[9] and Ivey[10]). The forces F_{zd} and V_{xd} were considered by Sulzberger.[11] A characteristic of all of these theoretical treatments is that the contributions to F_{xa} and F_{xb} of the shear stresses in the x direction along the sides of the footing have been neglected. Another factor which has not been previously considered is the development of shear stresses (V_{za} and V_{zb}) in the z direction due to the vertical movement of footing surface areas with respect to the surrounding soil.

The neglect of these forces has contributed to the conservatism of previous theoretical solutions. These factors will be considered in this analysis, which will be broken down according to the following outline:

I. Soil with Both Cohesion and Internal Friction.
   A. Lateral Forces F_{xa} and F_{xb}
      1. Distribution of compressive stresses around footing perimeter
      2. Distribution of shear stresses around footing perimeter
      3. Summation of components of stresses in x direction into F_{xa} and F_{xb}

[1]Terzaghi, Karl, "Theoretical Soil Mechanics," John Wiley & Sons, New York, 1963, p. 26.

[2]Ibid, pp. 26.

[3]Ibid, pp. 356.

[4]Seiler, J. F., "Effect of Depth of Embedment on Pole Stability," Wood Preserving News, Vol. 10, No. 11, November 1932.

[5]Patterson, Donald, "How to Design Pole Type Buildings," American Wood Preservers Institute, 1957, p. 13.

[6]Downs, Dallas I., et al., "Transmission Tower Foundations," Journal of the Power Division, **Proceedings ASCE**, April 1966, p. 91.

[7]Anderson, W. C., "Foundations to Resist Tilting Moments Imposed on Upright Candilevers Supporting Highway Signs," Highway Research Board, Bulletin 247, 1960.

[8]Will, Heinrick, "Zur Berechnung der Einspannung und des Spannungsverlaufes bei in das erdreich eingegrabenen Pfählen," Beton U. Eisen, 1911.

[9]Williams, Clement C., "The Design of Masonry Structures," McGraw-Hill Book Company, Inc., New York, 1930, p. 479.

[10]Ivey, Don L., and Hawkins, Leon, "Signboard Footings to Resist Wind Loads," Civil Engineering, December 1966, p. 34.

[11]Sulzberger, G., "Die Fundamente der Freilerlungs tragwerk und ihre Berechnung," Bulletins Association Suisse des Electriciens, Juni 1927.

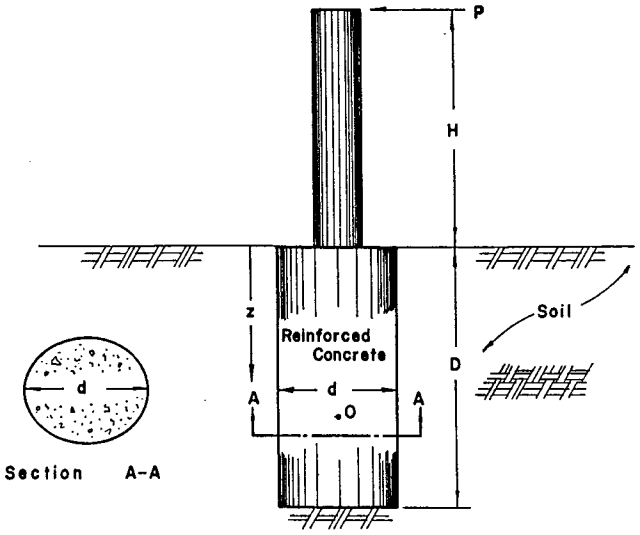

Figure 1. Drilled shaft footing subjected to an overturning load.

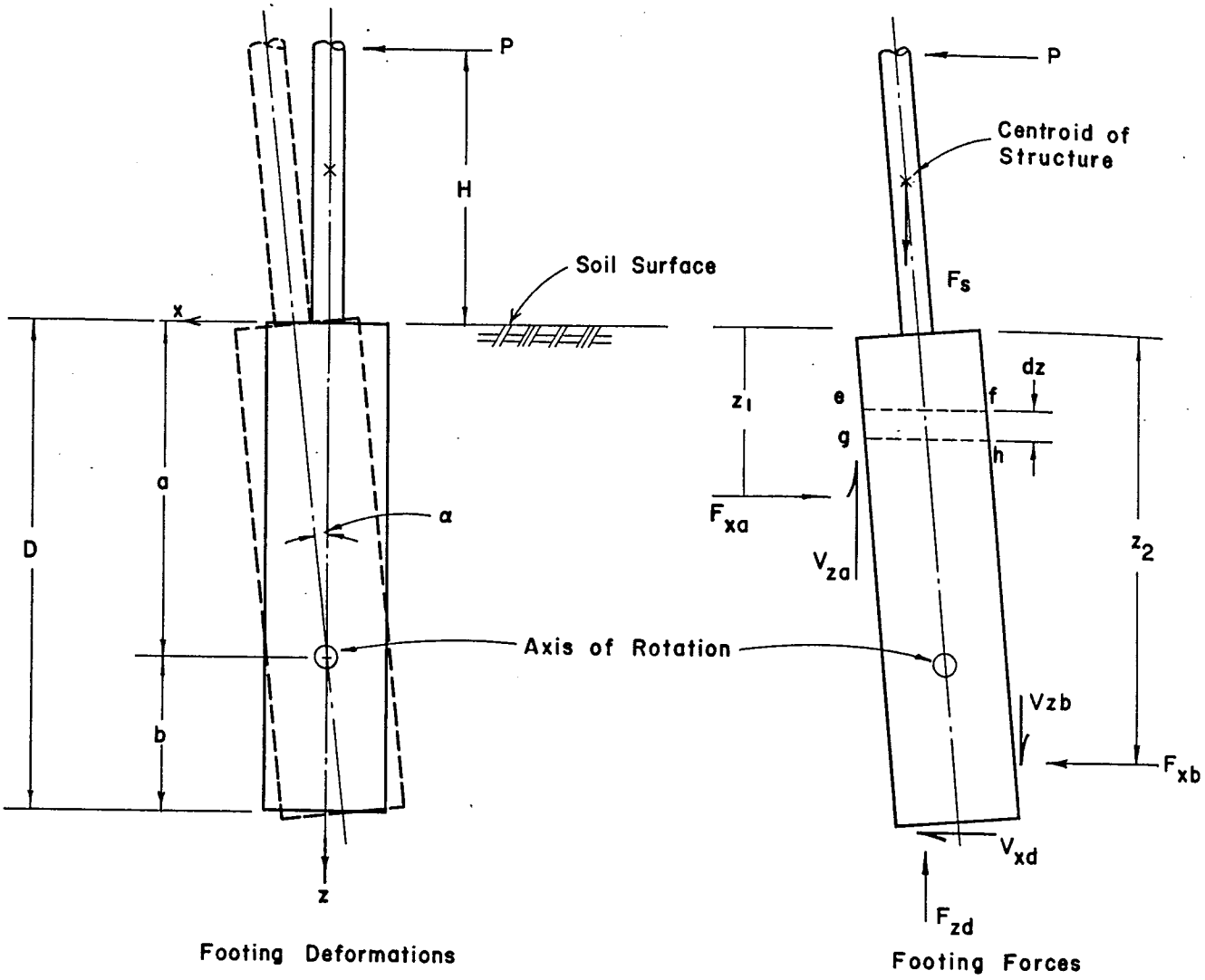

Figure 2. Soil deformations and footing forces developed by overturning load.

4. Contribution of F_{xa} and F_{xb} to moment about the Point $z = 0$

B. Vertical Shear Forces V_{za} and V_{zb}

1. Vertical movement (in the z direction) of points on the surface of the footing
2. Shear stress development on cylindrical surfaces
3. Summation of shear stresses into forces V_{za} and V_{zb}
4. Summation of shear stresses into a moment resisting overturning (M_v)

C. Forces on Bottom of Footing V_{xd} and F_{zd}

1. Determination of F_{zd}
2. Determination of V_{xd}

D. Development of equilibrium equations that can be solved to determine a footing's maximum resistance to overturning

II. Cohesionless Soil.
(Same development sequence as I.)

Procedure and Solution

Soil tested in such a way that there is cohesion but no apparent internal friction can be considered a special case of Part I with the angle of internal friction (ϕ) equal to zero. Cohesionless soil necessitates a separate treatment since active pressures on retreating surfaces of the footing are present.

In each case it will be assumed that the footing is surrounded by a homogeneous isotropic soil with known values of cohesion (c) and angle of internal friction (ϕ). The inherent nature of stratification makes it undesirable to formulate general equations which would encompass all the possibilities that could be encountered in practice. These problems must be treated on an individual basis using the same basic principles developed for uniform soils.

I. Soil with Both Cohesion and Internal Friction

A. Lateral Forces F_{xa} and F_{xb}

1. Distribution of compressive stresses around footing perimeter.

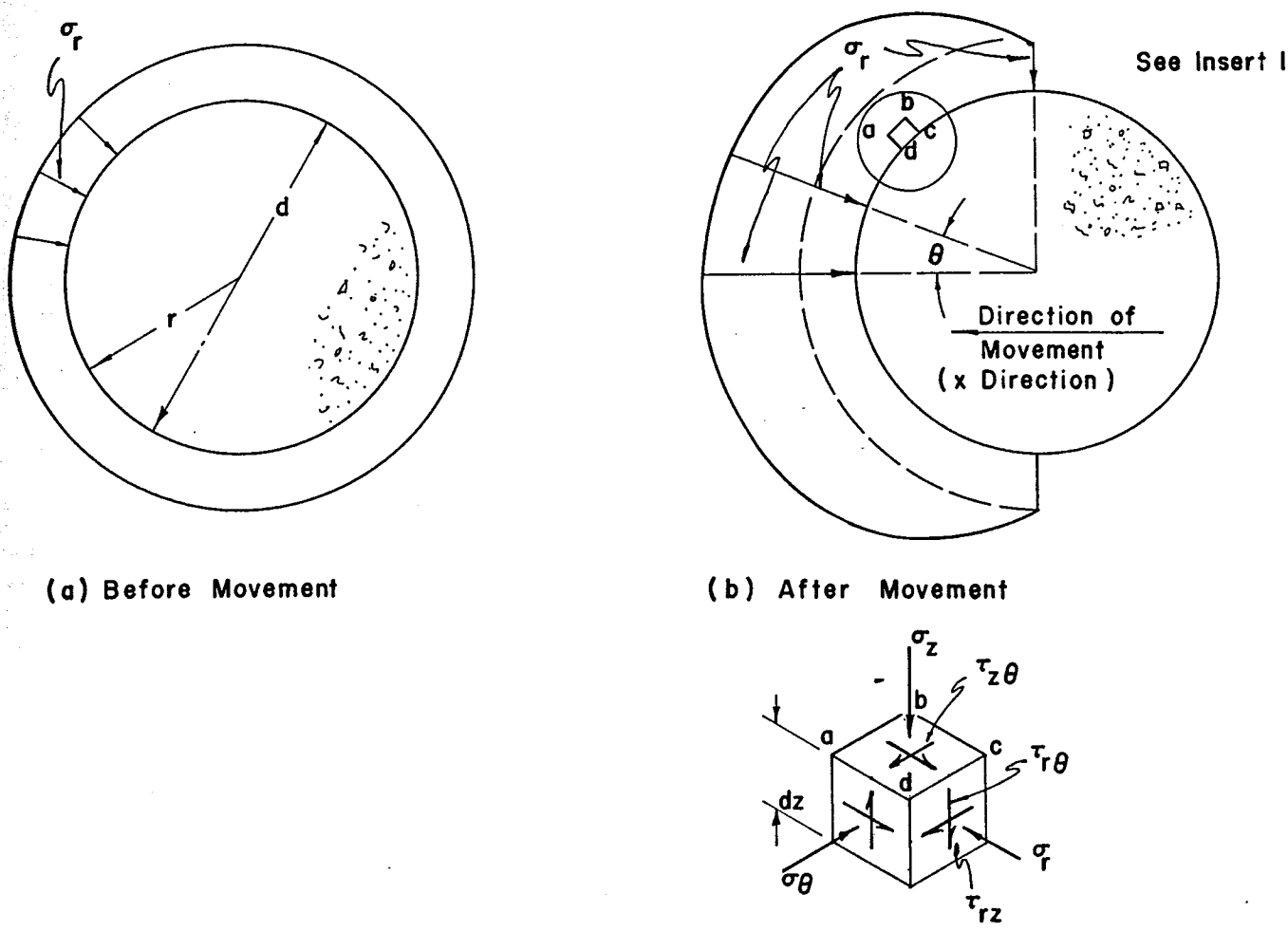

Figure 3. Soil stresses due to footing movement.

A segment of the footing at a depth z, cut out by two parallel planes which are perpendicular to the longitudinal axis of the cylinder, and a distance dz apart moves horizontally (in the x direction) in proportion to its distance from the axis of rotation (Figure 2). Viewing the segment from above, the stress conditions before and after movement are shown in Figure 3.

For this development cylindrical coordinates will be used, with positive values of Θ measured clockwise from the old x axis (the direction of movement) when viewed from above, and r defining points radially from the longitudinal axis of the footing. As before, the longitudinal footing axis is the z axis. The coordinate axis z is positive downward, with its origin at the top of the footing. Before movement of the footing, the stresses present are those of the horizontal earth pressure at rest. These stresses are defined by Terzaghi[12] as $K_o\gamma z$, where K_o is the coefficient of earth pressure at rest and γ is the unit weight of the soil. As horizontal movement of this segment takes place, the stresses increase on the advancing surface and are reduced on the receding surface. A maximum value of stress is encountered on the portion of the advancing surface at the point $\Theta = 0$. This maximum stress decreases in some manner to a value of the original pressure, $K_o\gamma z$ at $\Theta = \pi/2$ and $3\pi/2$.

It will be assumed that this maximum radial stress can be expressed as a function of depth, unit weight and cohesion in a Rankine[13] type equation,

$$\sigma_{r_{max}} = K_1\gamma z + K_2 c \qquad (1)$$

K_1 and K_2 are functions of the angle of internal friction

[12]Terzaghi, Karl, "Theoretical Soil Mechanics," John Wiley & Sons, New York, 1963, p. 29.

[13]Terzaghi, Karl, and Peck, Ralph B., "Soil Mechanics in Engineering Practice," John Wiley & Sons, New York, p. 149.

(φ), but not necessarily the same functions derived by Rankine for frictionless walls of semi-infinite length.

The pressure on the receding surface ($\pi/2 < \Theta < 3\pi/2$) is rapidly reduced to zero as the footing loses contact with the soil. For values of cohesion (over 500 psf), at the depths under consideration for this type of footing (under 10 ft.) positive active pressure does not exist.[14]

A cosine distribution of pressure along the advancing perimeter will be used to decrease the pressure from its maximum value of $K_1\gamma z + K_2 c$ to its minimum value of $K_o\gamma z$.

Thus,

$$\sigma_r = K_o\gamma z + [\,(K_1 - K_o)\,\gamma z + K_2 c\,]\cos\Theta \quad (2)$$

Some precedent has been established for this type of distribution in the solution of elasticity problems.[15] Since the plastic flow concept allows development of additional stresses in areas adjacent to the initial point of maximum stress, this cosine distribution is probably a conservative assumption.

2. Distribution of shear stresses around footing perimeter.

Considering the shearing stresses developed by the movement of the footing, it is apparent the greatest tendency for the development of shear in the Θ direction is at $\Theta = \pi/2$ and $3\pi/2$. Also apparent is the lack of any shear development at $\Theta = 0$. If the tendency for shear movement of the footing with respect to the soil is taken as the indicator of the development of shear stress, it is seen that a sine function of Θ could be used to describe this distribution.

Since the maximum shear stress[16] the soil can develop on this plane is

$$\sigma_r\tan\phi + c,$$

the distribution between $\Theta = 0$ and $\Theta = \pi/2$ will be assumed as

$$\tau_{r\theta} = (\sigma_r\tan\phi + c)\sin\Theta \quad (3)$$

3. Summation of components of stresses in the x direction into F_{xa} and F_{xb}.

The components of the stresses σ_r and $\tau_{r\theta}$ in the x direction can be integrated over the advancing perimeter of the footing segment, yielding the total resistance to movement in the x direction at any depth z.

or,

$$F_{xz} = 2\int_0^{\pi/2} \sigma_r\cos\Theta\, dA + 2\int_0^{\pi/2} \tau_{r\theta}\sin\Theta\, dA$$

where σ_r and $\tau_{r\theta}$ are defined by equations (2) and (3)

and $dA = r\, d\Theta\, dz$.

Integration yields

$$F_{xz} = 2\, r\, dz(\gamma z E) + cG), \quad (4)$$

where

$$E = K_o\left(1 + \frac{\pi}{4}\tan\phi - \frac{\tan\phi}{3} - \frac{\pi}{4}\right) + K_1\left(\frac{\pi}{4} + \frac{\tan\phi}{3}\right)$$

and

$$G = \frac{\pi}{4} + K_2\left(\frac{\pi}{4} + \frac{\tan\phi}{3}\right)$$

Then F_{xa} and F_{xb} are determined by

$$F_{xa} = \int_o^a F_{xz} \qquad F_{xb} = \int_a^D F_{xz}$$

Substitution and integration yields

$$F_{xa} = 2r\left[\gamma E\ \frac{a^2}{2} + c\,G\,a\right] \quad (5)$$

and

$$F_{xb} = 2r\left[\gamma E\ \frac{(D^2 - a^2)}{2} + cG\,(D - a)\right] \quad (6)$$

4. Contribution of F_{xa} and F_{xb} to the moment about the point, $z = 0$.

The moments due to F_{xa} and F_{xb} are defined by

$$F_{xa}\, z_1 = \int_0^a zF_{xz} \text{ and } F_{xb}\, z_2 = \int_a^D zF_{xz}$$

Substitution and integration yields

$$F_{xa}\, z_1 = 2r\left[\gamma E\ \frac{a^3}{3} + cG\ \frac{a^2}{2}\right] \quad (7)$$

and

$$F_{xb}\, z_2 = 2r\left[\gamma E\ \frac{D^3 - a^3}{3} + cG\ \frac{D^2 - a^2}{2}\right] \quad (8)$$

B. Vertical Shear Forces V_{za} and V_{zb}

1. Vertical movement (in the z direction) of points on the surface of the footing.

As shown in Figure 4, if the origin of coordinates, z, r and Θ is shifted down to the axis of rotation, the movement in the z direction of a point "i" due to a rotation about a — a′ of α can be expressed as

$$dz' = z' - z'\cos\alpha + r\cos\Theta$$

From this equation it is seen that all points on the surface above the axis of rotation from $\Theta = \pi/2$ to $\Theta = -\pi/2$ move downward, with the exception of the points $z = 0$, $\Theta = \pi/2$ and $z = 0$, $\Theta = 3\pi/2$. Simi-

[14] Terzaghi, Karl, "Theoretical Soil Mechanics," John Wiley and Sons, New York, 1953, pp. 37.

[15] Timoshenko, S., and Goodier, J. N., "Theory of Elasticity," McGraw-Hill Book Company, Inc., 1951, p. 113.

[16] Terzaghi, Karl, "Theoretical Soil Mechanics," John Wiley and Sons, New York, 1953, p. 7.

larly, points on the surface below the axis of rotation between the value of $\Theta = \pi/2$ and $\Theta = 3\pi/2$ move upward.

2. Shear stress development on cylindrical surfaces.

Due to this movement of the footing with respect to the soil, the shear stresses shown in Figure 5 are induced. As in the case of radial stresses the loss of contact between the footing and the soil dictates that the shear stresses are zero on the areas indicated. As indicated before, the maximum value these stresses can achieve is

$$\sigma_r \tan\phi + c,$$

but they cannot fully approach this condition on surfaces of the footing that already have a significant circumferential shear stress ($\tau_{r\theta}$). In consideration of this a reduction factor (J_1) is used to estimate the effect of this shearing stress.

Thus,

$$\tau_{rz} = J_1 (\sigma_r \tan\phi + c) \qquad (9)$$

For very stiff cohesive materials, which allow only a small rotation before reaching ultimate load, J_1 will probably approach zero. For a highly plastic material it will take some value between zero and one.

3. Summation of shear stresses into forces V_{za} and V_{zb}.

The force V_{za} shown in Figure 2 can be found by integrating the stresses on the surface above the axis of rotation.

$$V_{za} = 2 \int_0^a \int_0^{\pi/2} \tau_{rz} \, dA$$

Similarly,

$$V_{zb} = 2 \int_a^D \int_0^{\pi/2} \tau_{rz} \, dA$$

The difference in V_{za} and V_{zb} which will be of interest later will be called F_v.

$$F_v = V_{za} - V_{zb}$$

Substitution and integration yield

$$F_v = 2J_1 r \left[\tan\phi \left(\frac{\pi}{2} K_o \gamma + (K_1 - K_o)\gamma \right) \right. \qquad (10)$$

$$\left(a^2 - \frac{D^2}{2} \right) + \left(K_2 \, c \tan\phi \right.$$

$$\left. \left. + c \, \frac{\pi}{2} \right) (2a - D) \right]$$

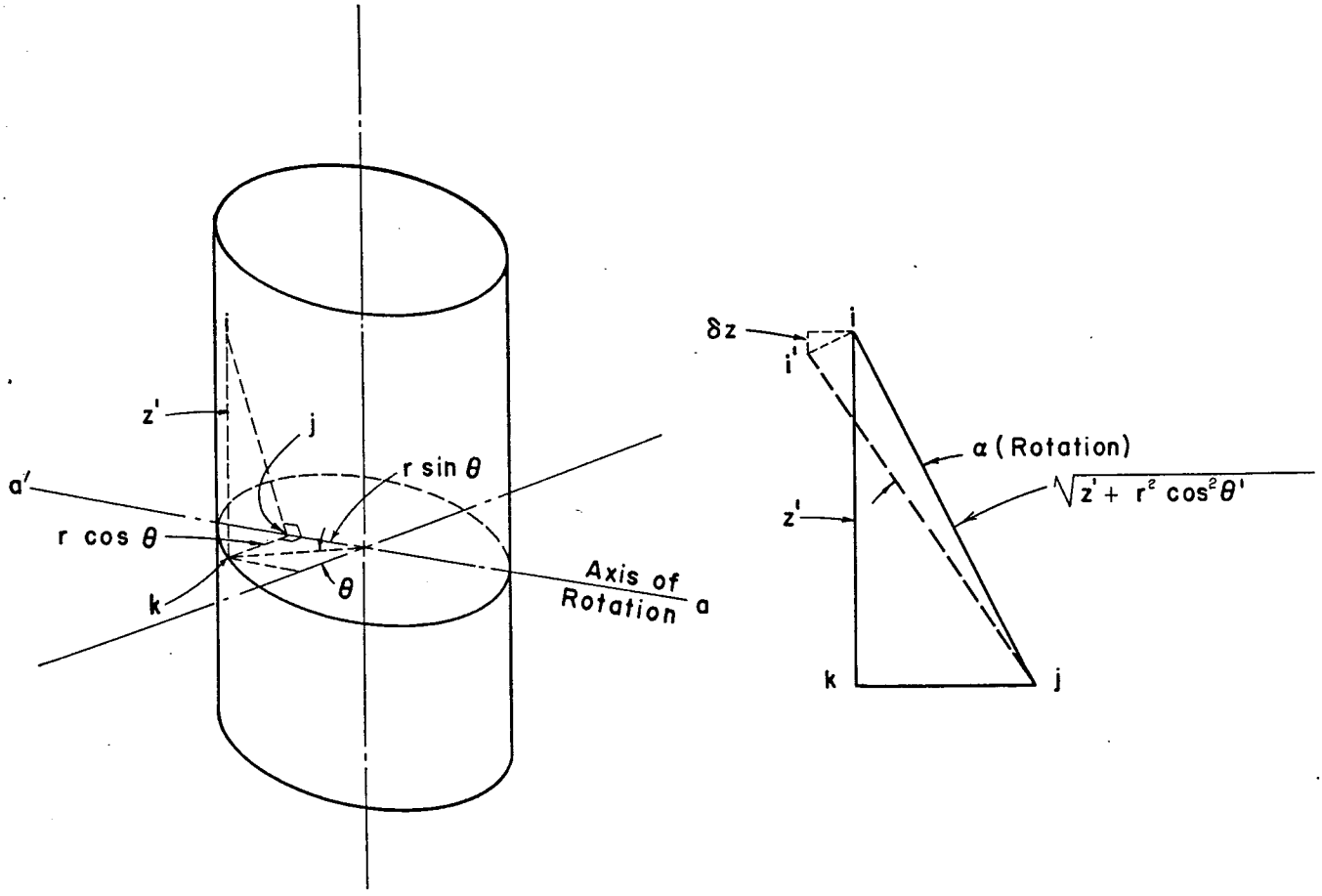

Figure 4. Vertical movements of points on surface of footing.

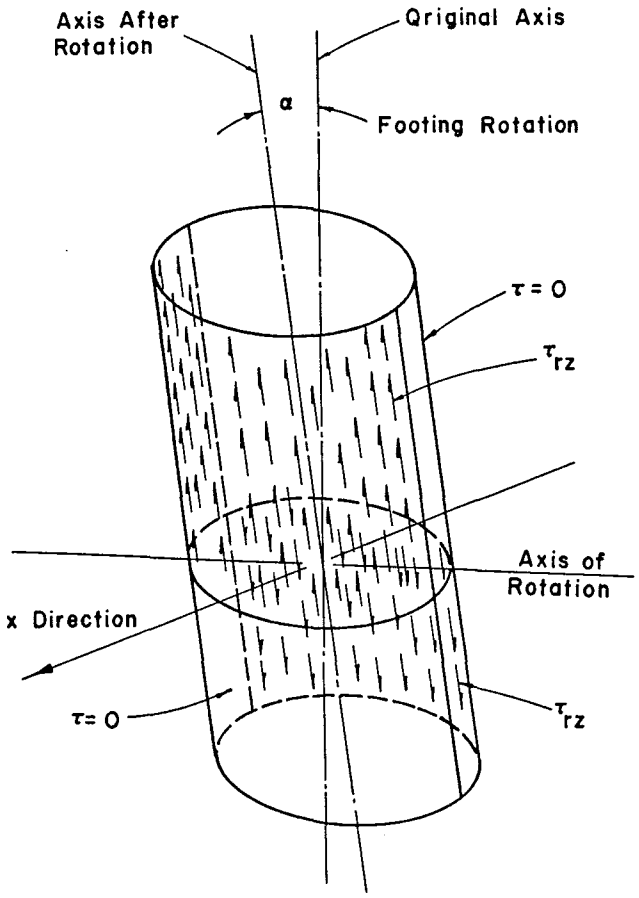

Figure 5. Vertical shear stresses.

4. Summation of shear stresses into a moment resisting overturning. (Mv)

The summation of all τ_{rz} dA's times their individual moment arms ($\bar{m}$) about the axis of rotation can be found by integration, yielding a moment resisting overturning (M_v).

Thus,

$$M_v = \int_{SURFACE} \int \bar{m}\ \tau_{rz}\ dA\ ,$$

or

$$M_v = 2 \int_0^a \int_0^{\frac{\pi}{2}} \bar{m}\ \tau_{rz}\ dA + 2 \int_a^D \int_0^{\frac{\pi}{2}} \bar{m}\ \tau_{rz}\ dA$$

which reduces to

$$M_v = 2r^2 J_1 (\gamma U + cW) \qquad (11)$$

where

$$U = \frac{\tan\phi D^2}{8} \left(K_o (4 - \pi) + K_1 \pi \right)$$

$$W = D \left(\frac{\pi}{4} K_2 \tan\phi + 1 \right)$$

C. Forces on Bottom of Footing, V_{xd} and F_{zd}.

1. Determination of F_{zd}

F_{zd} is determined by a summation of forces vertically.

$$F_{zd} = F_s - F_v = F_s + V_{zb} - V_{za} \qquad (12)$$

where F_s is the total weight of the structure on the footing plus the weight of the footing. $V_{za} - V_{zb}$ was previously defined in Section I, B.3. as F_v.

If any significant tilt (α) of the footing occurs, approximately half of the base of the footing will push into the soil while the other half will tilt upward, losing contact with the ground. This is shown by Figure 6. The exact distribution of pressure over this half of the circular bottom is of academic interest, probably approaching a maximum value close to the outer edge about point "P_1", and a minimum value close to line c — c', in the bottom view.

2. Determination of V_{xd}.

Having solved for the vertical force F_{zd} the shear force on the base of the footing will be due to the friction and the cohesion on the contact area.

The maximum value this force can achieve is then

$$F_{zd} \tan\phi + c \frac{\pi r^2}{2}$$

Since the maximum stress takes place at a rotation considerably less than that associated with ultimate load, the stress at ultimate load may be considerably less than maximum depending to a large degree on whether or not the soil is at critical density. Therefore, the modifying factor of J_2 is used.

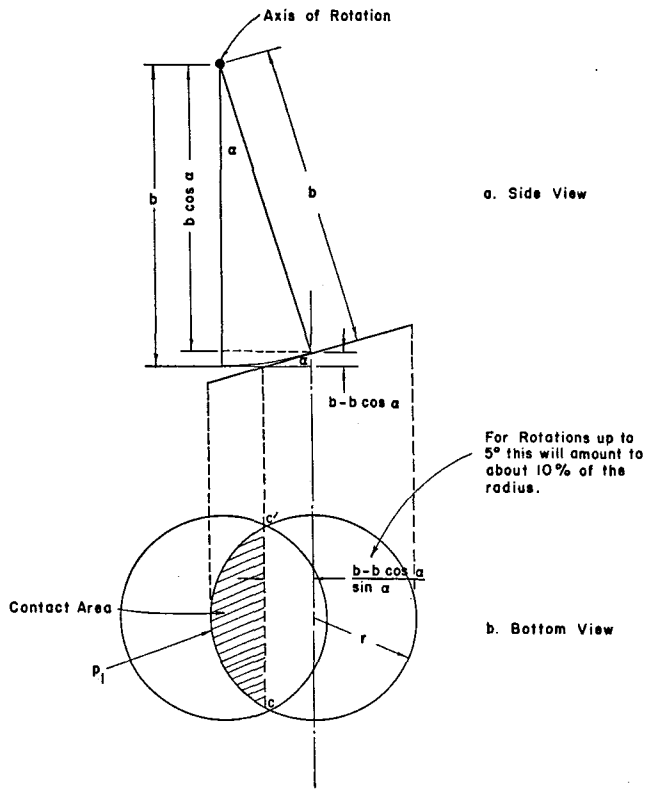

Figure 6. Contact area on base of footing due to rotation.

$$V_{xd} = J_2 \left(F_{zd} \tan \phi + c \frac{\pi r^2}{2} \right) \qquad (13)$$

D. Development of Equilibrium Equations.

Two equations are available to solve for the two unknowns in the previous developments; a, the distance down to the axis of rotation, and P_m, the maximum load. These are the summation of forces in the horizontal direction, and the summation of moments in the plane of rotation, respectively

Referring back to Figure 2,

$$\sum F_H = 0 \quad F_{xa} = P_m + F_{xb} + V_{xd} \qquad (14)$$

and

$$\sum M_{z=o} = 0 \quad P_m H + F_{xa} z_1 = M_v + F_{xb} z_2 + V_{xd} D \qquad (15)$$

The contributions of F_{zd} and F_s to the moment equation are dependent on the rotation (α). As the applied load increases toward its maximum value (P_m) the lines of action of F_{zd} and F_s approach coincidence. This is true in the range of d/D ratios of practical interest. Therefore, they can be neglected in the interest of making P_m independent of α.

Substitution of the previously defined terms into the equilibrium equations result in equations which can be solved for the distance down to the rotation point (a) and the maximum load (P_m).

II. Cohesionless Soil

The basic difference in the development of a theory for cohesionless soils is that there is active pressure ($K_A \gamma z$) on the portion of the footing retreating from the soil mass as well as the passive pressure on the advancing portion of the footing. The existence of these radial active pressures necessitates the consideration of the shearing stresses, $\tau_{r\theta}$ and τ_{rz} on these retreating surfaces as well as on the advancing surfaces. Figure 7 shows the resultant forces that must be evaluated to solve the problem.

A. Lateral Forces F_{xa} and F_{xb}.

1. Distribution of compressive stresses around footing perimeter.

Figure 8 illustrates the distribution of radial stresses on a segment of the footing at depth z moving through the soil. Using the same procedure as the cohesive development, the radial stress on the surface of the footing can be defined as follows.

from $\Theta = 0$ to $\Theta = \pm \frac{\pi}{2}$

$$\sigma_{r_f} = K_o \gamma z + (K_p - K_o) \gamma z \cos \Theta \qquad (1')$$

and from $\Theta = \frac{\pi}{2}$ to $\Theta = \frac{3\pi}{2}$

$$\sigma_{r_r} = K_o \gamma z - (K_o - K_A) \gamma z \cos \Theta \qquad (2')$$

The second subscript f or r denotes front and rear of the footing if the front is considered the advancing portion and rear the retreating portion. Thus the f side and r side switch as the portion below the axis of rotation is considered.

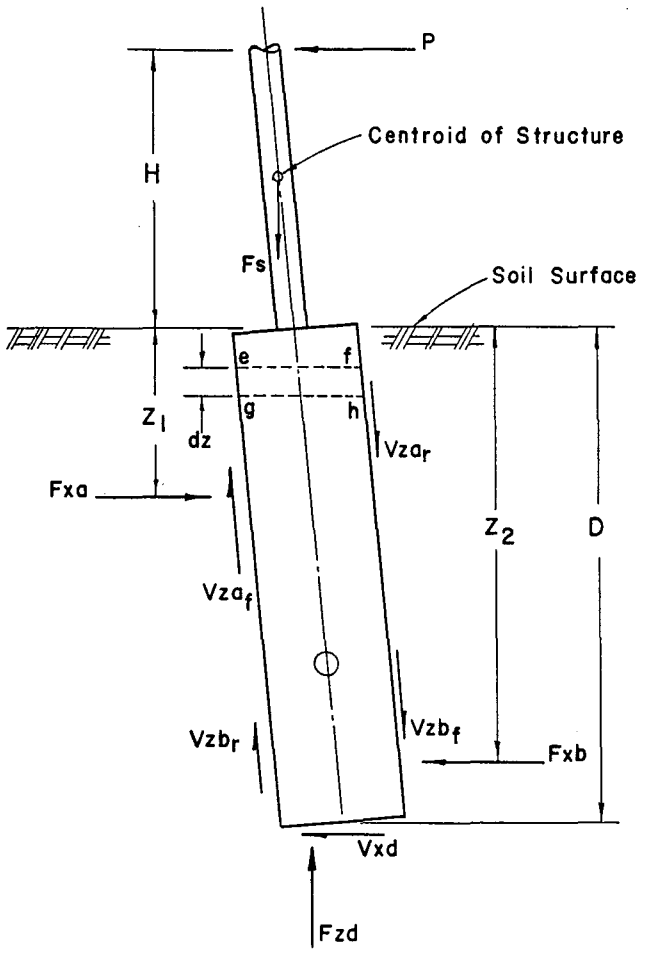

Figure 7. Footing forces developed by overturning load, cohesionless soil.

2. Distribution of shear stresses around footing perimeter.

$\tau_{r\theta}$ was defined previously in the cohesive development. Thus,

$$\tau_{r\theta_f} = \sigma_{r_f} \tan \phi \sin \Theta \qquad (3')$$

and

$$\tau_{r\theta_r} = \sigma_{r_r} \tan \phi \sin \Theta \; . \qquad (4')$$

3. Summation of components of stresses in x direction into Fxa and Fxb.

The resistance to movement in the x direction of a segment of thickness dz at depth z is given by the summation of forces due to σ_r and $\tau_{r\theta}$.

These summations are:

$$F_{x\sigma_r} = 2 \int_0^{\pi/2} \sigma_{r_f} \cos \Theta \, dA - 2 \int_0^{\pi/2} \sigma_{r_r} \cos \Theta \, dA \qquad (5')$$

Top View of Segment efgh of Figure 7

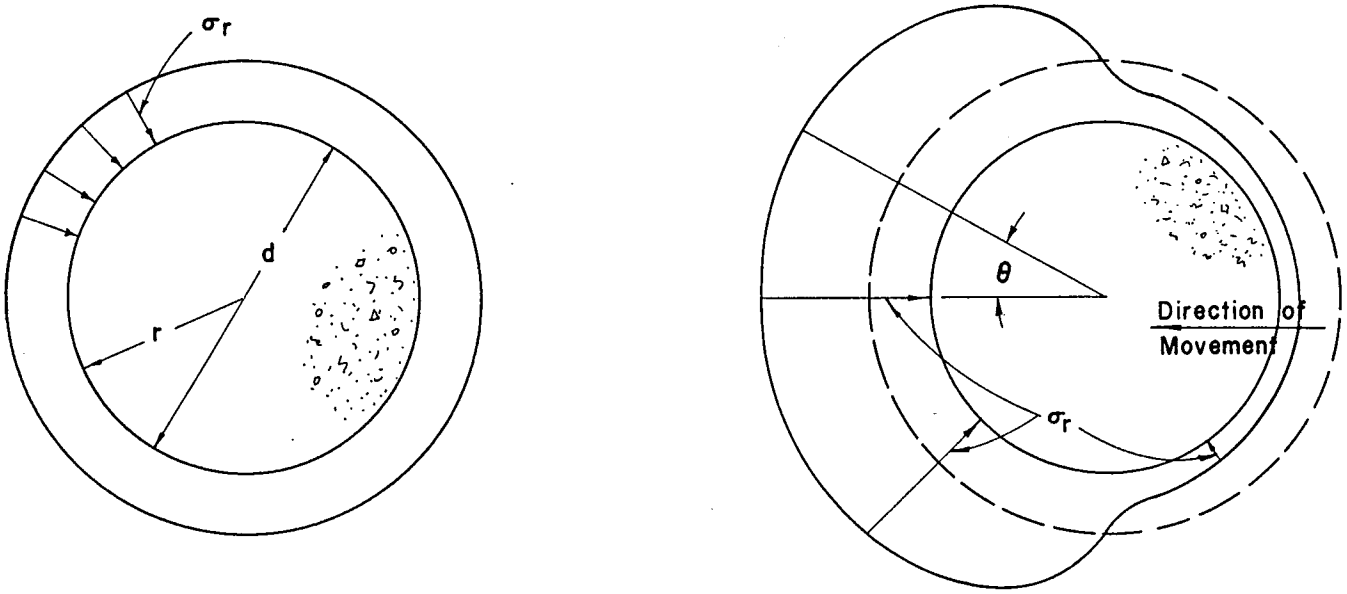

(a) Before Movement (b) After Movement

Figure 8. Cohesionless soil stresses due to footing movement.

$$F_{x\tau_{r\theta}} = 2 \int_0^{\pi/2} \tau_{r\theta_f} \sin\Theta \, dA + 2 \int_0^{\pi/2} \tau_{r\theta_r} \sin\Theta \, dA \qquad (6')$$

The radial stress (σ_{r_r}) on the retreating portion of the footing is contributing to movement, while the shear stress it produces ($\tau_{r\theta_r}$) is resisting movement.

The resulting force is then defined by equation 7'.

$$F_{xz} = F_{x\sigma_r} + F_{x\tau_{r\theta}} \qquad (7')$$

Substitution and integration yields:

$$F_{xz} = L \, z \, dz \qquad (8')$$

where

$$L = r\gamma \left[\frac{\pi}{2} (K_p - K_A) + 2 \tan\phi \left(K_o \left(\frac{\pi}{2} - \frac{2}{3} \right) + \frac{1}{3} (K_p + K_A) \right) \right]$$

Now F_{xa} is the summation of these forces over the portion of the footing down to the axis of rotation (from z = 0, to z = D) and F_{xb} is the summation below the rotation point (from z = a to z = D)

Thus

$$F_{xa} = \int_0^a F_{xz} = \int_0^a L \, z \, dz = \frac{La^2}{2} \qquad (9')$$

and

$$F_{xb} = \int_a^D F_{xz} = \int_a^D L \, z \, dz = \frac{L(D^2 - a^2)}{2} \qquad (10')$$

4. Contribution of the Fxa and Fxb to moment about the point z = 0.

The contribution of these forces to the moment about z = 0 is

$F_{xa} \, z_1$ and $F_{xb} \, z_2$,

where

$$F_{xa}z_1 = \int_o^a z \, F_{xz} = \int_0^a L \, z^2 \, dz = \frac{La^3}{3} \qquad (11')$$

and

$$F_{xb} \, z_2 = \int_a^D z \, F_{xz} = L \, \frac{(D^3 - a^3)}{3} \, . \qquad (12')$$

B. Vertical Shear Forces V_{za_f}, V_{zb_f}, V_{za_r} and V_{zb_r}.

1. Same as I B.1
2. Same as I B.2
3. Summation of shear stresses into forces.

The four vertical shear forces shown in Figure 7 will be treated. Using the same arguments as in the cohesive development, let

$$\tau_{rz} = J_1 \sigma_r \tan \phi \qquad (13')$$

Then

$$V_{za_f} = 2 \int_0^a \int_0^{\pi/2} \tau_{rz_f} \, dA$$

$$V_{zb_r} = \int_a^D \int_0^{\pi/2} \tau_{rz_r} \, dA$$

and

$$V_{za_r} = 2 \int_0^a \int_0^{\pi/2} \tau_{rz_r} \, dA$$

$$V_{zb_f} = \int_a^D \int_0^{\pi/2} \tau_{rz_f} \, dA$$

The total vertical force (F_v) is equal to

$$V_{za_f} + V_{zb_r} - V_{za_r} - V_{zb_f}$$

Substitution and integration yields

$$F_v = J_1 \, r \tan \phi \, \gamma (K_p - K_A) \, \frac{(3a^2 - D^2)}{2} \qquad (14')$$

4. Summation of vertical shear stresses into a moment resisting overturning (M_v).

The contribution of each segment of the footing (i.e., above or below the axis of rotation and on the front or rear) will be determined by:

$$M_{za_f} = 2 \int_0^a \int_0^{\pi/2} \overline{m} \, \tau_{rz_f} \, dA$$

$$M_{zb_r} = 2 \int_0^D \int_0^{\pi/2} \overline{m} \, \tau_{rz_r} \, dA$$

$$M_{za_r} = 2 \int_0^a \int_0^{\pi/2} \overline{m} \, \tau_{rz_r} \, dA$$

$$M_{zb_f} = 2 \int_0^D \int_0^{\pi/2} \overline{m} \, \tau_{rz_f} \, dA$$

The total moment M_v is then defined by

$$M_v = M_{za_f} + M_{zb_r} + M_{za_r} + M_{zb_f}$$

Substitution and integration yields

$$M_v = r^2 D^2 \gamma J_1 \tan \phi \left[K_o \left(2 - \frac{\pi}{2} \right) + \frac{\pi}{4} (K_p + K_A) \right] \qquad (15')$$

C. Forces on Bottom of Footing, V_{xd} and F_{zd}.

1. Determination of F_{zd}.

V_{xd} and F_{zd} are shown in Figure 7. F_{zd} is determined by the summation of forces vertically.

$$F_{zd} = F_s - F_v$$

Where F_s is the total weight of the structure on the footing. F_v is the unbalance in the vertical shear stresses defined by Equation 14'.

The maximum value V_{xd} can then assume is defined by

$$V_{xd} = F_{zd} \tan \phi$$

Since the base of the footing has already reached and passed this maximum value before the maximum footing resistance is reached[17] (the ultimate lateral forces F_{xa} and F_{xb} develop more slowly) this value of V_{xd} should be modified by the factor J_2.

Thus

$$V_{xd} = J_2 \, F_{zd} \tan \phi \qquad (16')$$

D. Development of Equilibrium Equations.

The summation of forces in the horizontal (x) direction (Equation 17') and the summation of moments in the plane of the footing rotation (Equation 18') are the conditions necessary to solve for a, the distance down to the point of rotation, and P_m, the ultimate load.

$$\sum F_H = 0, \; F_{xa} = P_m + V_{xd} + F_{xd} \qquad (17')$$

$$\sum M_{z=o} = 0, \; M_v + F_{xb} z_2 + V_{xd} \, D = P_m H + F_{xa} z_1 \qquad (18')$$

[17] Sulzberger, G., "Die Fundamente der Freileitunostragwerke und ihre Berechnung," Bulletin, Association Suisse Des Electriciens, June 1927.

SUMMARY

The application of the theory developed in this paper to engineering problems will depend on the accurate evaluation of the various soil coefficients by footing tests. This evaluation is a common characteristic of almost all applied theory in soil mechanics.

The coefficients of active and passive earth pressure (K_1, K_2, K_p and K_A) have been previously defined by Rankine[18] for the case of frictionless walls of semi-infinite length. They are given as the following functions of the angle of internal friction (ϕ).

$$K_1 = K_p = \tan^2 \left(45 + \frac{\phi}{2} \right)$$

$$K_2 = 2 \tan \left(45 + \frac{\phi}{2} \right)$$

$$K_A = \tan^2 \left(45 - \frac{\phi}{2} \right)$$

Since the problem under consideration is not the same as Terzaghi's because of footing friction and the relatively narrow footing width, it would not be expected that the same coefficients would be applicable. One possible solution would be for one or more of them to be modified by an empirically determined multiplication factor. This factor may prove to be a function of the particular soil characteristics.

Other coefficients such as J_1, J_2 and K_o, which have a possible variation of 0 to 1.0 may prove to have a relatively small effect on the solution for ultimate load. By checking the sensitivity of the solution to variations in these coefficients, and by comparison with actual footing test data, values may be chosen which will need little modification over wide variations in soil properties.

In considering the solution of the equilibrium equations which are derived, (Equations 14 and 15 for cohesive soil and 17′ and 18′ for cohesionless soil) the elimination of one of the unknowns (a or P_m) will result in a cubic equation in the other unknown. Since the equation is quite cumbersome, the problem has been programmed for the IBM 7094. This program is now being used to check the sensitivity of the solution to the various soil parameters. Thirty model tests have been run on soils varying from cohesionless sands to highly plastic clays as another part of this study. The theory will be compared to these tests in Research Report 105-2.

[18]Terzaghi, Karl, "Theoretical Soil Mechanics," John Wiley and Sons, New York, pp. 30 and 38.